DOI: 10.1002/cphc.200800751

Exciton Binding Energies in Conjugated Polyelectrolyte Films

Jung Hwa Seo,[a] Youngeup Jin,[b] Jacek Z. Brzezinski,[a] Bright Walker,[a] and Thuc-Quyen Nguyen*[a]

Conjugated polyelectrolytes (CPEs) are materials that have a conjugated backbone and charged functional groups. They are finding applications in optoelectronic devices such as light emitting diodes (LEDs),[1] solar cells,[2] light-emitting electrochemical cells,[3] and optically amplified biosensor assays.[4] Since the ionic groups increase solubility in polar solvents such as water or alcohols, CPEs enable fabrication of multilayer organic LEDs (OLEDs) using solution-casting methods when combined with neutral conjugated polymers.[2,5] Solution processing techniques such as inkjet printing, roll-to-roll coating, and screen-printing reduce fabrication costs, when compared to inorganic semiconductors.[6] The CPE function in these OLEDs is that of electron injection/transport layers (EILs/ETLs) and allows the use of stable metals as cathodes, potentially simplifying the encapsulation process.[1,5a]

Recent studies have shown that the performance of OLEDs based on CPEs depends strongly on the charge-compensating counterions, the charge type and the backbone structure.[5a,7] There has been a general acceptance that the pendant ionic functionalities have no influence on the electronic structure of the backbone.[1d,8] However, ultraviolet photoelectron spectroscopy (UPS) results have recently shown that CPE with similar backbones but different counterions have markedly different ionization potentials (IP), electron affinities (EA) and vacuum levels, which are intimately related to the charge injection barrier.[9] A detailed understanding of CPE electronic structure as a function of these structural variables is therefore important. However, there have been few efforts to empirically study it due to the difficulty of interpretation and analysis of conjugated polymers with long chains and various degrees of intermolecular interactions.[10,11]

To construct the energy diagrams of organic semiconductors, the lowest unoccupied molecular orbital (LUMO) is usually estimated from the optical gap (E^{opt}), as measured by UV/Vis absorption and the highest occupied molecular orbital (HOMO) is obtained by cyclic voltammetry (CV) or UPS.[1d,12]

However, the E^{opt} is often smaller than the transport gap (E^{T}) due to the interaction between the electron–hole pair (exciton effect), as shown in Figure 1. The transport gap is defined by

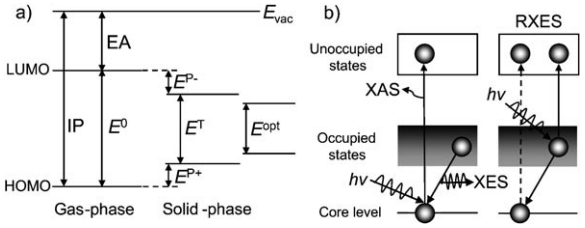

Figure 1. a) Left: The ionization potential (IP) and electron affinity (EA) of a gas-phase molecule with an energy gap E^0. Center: Relaxed polaron levels including the polarization energies E^{P+} for cations ("hole") and E^{P-} for anions ("electron") in a charged molecule. Right: the optical gap (E^{opt}) for the neutral excited molecule. b) In X-ray absorption spectroscopy (XAS), a core electron is excited to the unoccupied states, when X-ray is incident. Here, the photons measured in X-ray emission spectroscopy (XES) are produced when electrons in the occupied states refill the core hole. The energy loss in resonant XES (RXES) typically corresponds to the transitions in which electrons in the occupied states are scattered to the unoccupied states when excitation energy is tuned near or on-threshold. (E_{vac}: vacuum level, E_F: Fermi level).

the existence of free electron-hole pairs. For this reason, it can result in an error equal to the exciton binding energy ($E^{exciton}$).[13] It has been reported that in conjugated polymers, the $E^{exciton}$ is small (~200 meV), while in small molecules such as C_{60}, the $E^{exciton}$ is larger (~1 eV).[14] Until now, the $E^{exciton}$ of CPEs has remained unknown. Generally, a large $E^{exciton}$ is desirable in OLEDs to increase the probability of electron-hole pair recombination, while a small $E^{exciton}$ is required in solar cells to facilitate the charge generation via ultrafast electron transfer. Moreover, it is known that the interfacial dipoles (~0.5 eV) of two cationic CPEs are larger than the neutral and anionic CPE conterparts.[9] The large interfacial dipole in organic semiconductors can arise from the orientation of permanent dipoles. However, it is generally not straightforward to experimentally determine the dipole moment at an interface, particularly for disordered polymeric systems.[15,16] Overall, the determination of E^{T}, $E^{exciton}$ and the molecular dipole moment (***P***) is essential for a deep understanding of carrier injection, charge generation and transport phenomena in conjugated polymers.

In this contribution, we employ X-ray absorption spectroscopy (XAS) and X-ray emission spectroscopy (XES) to determine the E^{T} directly and estimate the LUMO and $E^{exciton}$. Figure 1b depicts schematically the XAS process. Absorption of an X-ray photon promotes an electron from the core level to an unoccupied state, leaving behind a hole in the core level. XAS thus reveals information about LUMO levels.[17] In XES, an emitted photon is detected when an electron in the occupied valence states refill a core hole, providing information on the HOMO levels.[18] The use of resonant XES (RXES) allows also selecting specific atomic species in the CPEs and probing local energy structure by tuning the incident photon energy to certain elec-

[a] *Dr. J. H. Seo, Dr. J. Z. Brzezinski, B. Walker, Prof. T.-Q. Nguyen*
Center for Polymers and Organic Solids
Department of Chemistry and Biochemistry
University of California, Santa Barbara, CA 93106 (USA)
Fax: (+1) 805-893-4120
E-mail: quyen@chem.ucsb.edu

[b] *Dr. Y. Jin*
Department of Chemistry
Pusan National University, Busan (Korea)

Supporting information for this article is available on the WWW under http://dx.doi.org/10.1002/cphc.200800751.

tronic transitions.[19] We investigated in our studies a set of CPEs with an identical poly(fluorene-*co*-phenylene) backbone structure but with different counterions and charges. As shown in Scheme 1, the materials are poly[9,9-bis[6′-(*N,N,N*-tri-

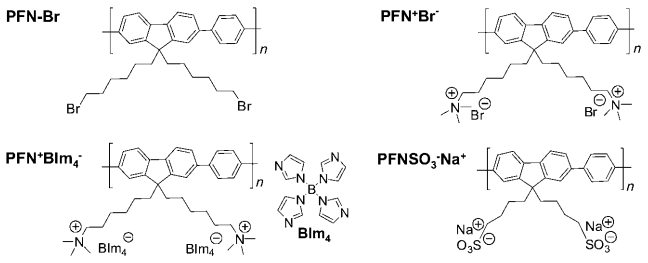

Scheme 1. Chemical structures of **PFN-Br**, **PFN$^+$Br$^-$**, **PFN$^+$Blm$_4^-$** and **PFNSO$_3^-$Na$^+$**.

methylammonium)hexyl]fluorene-*alt*-*co*-1,4-phenylene]bromide (**PFN$^+$Br$^-$**), the neutral precursor of **PFN$^+$Br$^-$** (**PFN-Br**), poly-[9,9-bis[6′-(*N,N,N*-trimethylammonium)hexyl] fluorene-*alt*-*co*-1,4-phenylene] tetrakis (imidazoly) borate (**PFN$^+$Blm$_4^-$**), and sodium poly[9,9-bis(4′-surfonatobutyl)fluorene-*alt*-*co*-1,4-phenylene] (**PFNSO$_3^-$Na$^+$**). From the distance between the HOMO and LUMO energy positions obtained from XES and XAS experiments, the E^T of CPEs can be directly determined (Figure 1). We have also evaluated the $E^{exciton}$ of CPEs by subtracting E^{opt} from E^T.[13,15] Additionally, considerable insight into the ***P*** of CPEs is gained from density functional theory (DFT).[16a,20]

Figure 2a shows the C 1s XAS spectra of **PFN-Br**, **PFN$^+$Br$^-$**, **PFN$^+$Blm$_4^-$** and **PFNSO$_3^-$Na$^+$**. All XAS spectra are normalized to the peak at 300 eV after matching the baselines at 280 eV. The sharp peaks observed below 292 eV correspond to C 1s→

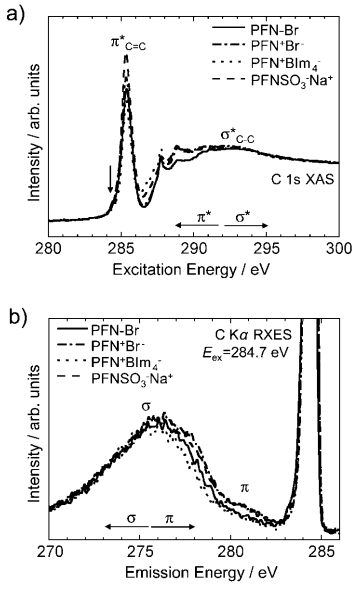

Figure 2. a) Normalized C 1s XAS spectra show π* and σ* resonances in the unoccupied electronic states. b) C Kα RXES spectra show π and σ transitions from C 1s in the occupied electronic states. The strong feature is taken at the excitation energy (E_{ex}) of 284.7 eV, which is the first π* resonance (denoted as an arrow) in Figure 2a.

π* transitions (π* resonance), while the broader structures observed above 292 eV correspond to C 1s→σ* transitions (σ* resonance).[21] From the asymmetry of the $\pi^*_{C=C}$ peak around 285 eV, one can surmise that additional features appear at the shoulder (denoted as an arrow). The peak at 287.7 eV in the four polymers corresponds also to a mixture of Rydberg and hydrogen-derived antibonding molecular orbital states of σ^*_{C-H} and π^*_{C-H}.[22] In addition, C 1s→π* transitions between 286 and 288 eV are observed in the spectra of **PFN$^+$Blm$_4^-$** (dot line) and **PFNSO$_3^-$Na$^+$** (dash line). The overall spectral features agree well with near edge X-ray absorption fine structure (NEXAFS) spectra previously reported for poly[9,9-bis[6′-(*N,N,N*-trimethylammonium)hexyl]fluorene (**PF**) derivatives.[22] All CPEs exhibit four similar features in the π* resonance region (the LUMO regions), even though their relative intensities at 283–292 eV are different. The π* resonances are also explained by various contributions of electronic transitions from the C 1s states from chemically different C atoms. Although the positions and shapes of the absorption features are similar, the spectral intensity from each resonance and the presence of certain shoulders reflect different molecular orderings and electronic transitions into the CPE LUMO levels.

The C Kα RXES spectra of **PFN-Br**, **PFN$^+$Br$^-$**, **PFN$^+$Blm$_4^-$** and **PFNSO$_3^-$Na$^+$** are presented in Figure 2b. All RXES spectra were calibrated with respect to the resonance peak of 284.7 eV, which corresponds to the excitation energy (E_{ex}) for the first π* resonance observed in the C 1s XAS spectra. The spectral weight above 276 eV changes upon using different counterions and is contributed from π states (the HOMO region), while the σ states below 276 eV are insensitive to the different counterions. In the π state region (276–283 eV), the spectral onsets of **PFN$^+$Br$^-$** and **PFNSO$_3^-$Na$^+$** exhibit higher emission energies than that of **PFN-Br**, indicating higher HOMO energy positions (closer to the vacuum level). In contrast, **PFN$^+$Blm$_4^-$** exhibits a lower emission energy than that of **PFN-Br**, indicating a lower HOMO energy position (further away from the vacuum level). These observations are in agreement with previous UPS data, since **PFN$^+$Blm$_4^-$** has the highest hole injection barrier at **PFN$^+$Blm$_4^-$**/Au interface among the three CPEs.[9] One concludes that the CPE HOMO levels are modified from that of the neutral polymer depending on the type of counterions and charges.

The E^T for the CPEs is now evaluated from the XAS and XES results. The energy gaps determine optoelectronic properties in the solid state. Two types of energy gaps, such as E^T and E^{opt}, need to be considered and it is important to make a clear distinction between them. In polymer solids, E^T is the energy difference between the removal of an electron from the HOMO and the addition of an electron into the LUMO. E^{opt} corresponds to the formation of a Frenkel exciton with the electron and the hole on the same molecule or a charge transfer exciton with the electron-hole pair on two adjacent molecules. Therefore, a comparison of E^T with E^{opt} leads to an approximation of the $E^{exciton}$ ($=E^T-E^{opt}$), as shown in Figure 1a.

Combining XAS (unoccupied states) and XES (occupied states) results provides a method to determine the E^T.[13,20] Figure 3a presents the C 1s XAS (filled circle) and C Kα XES

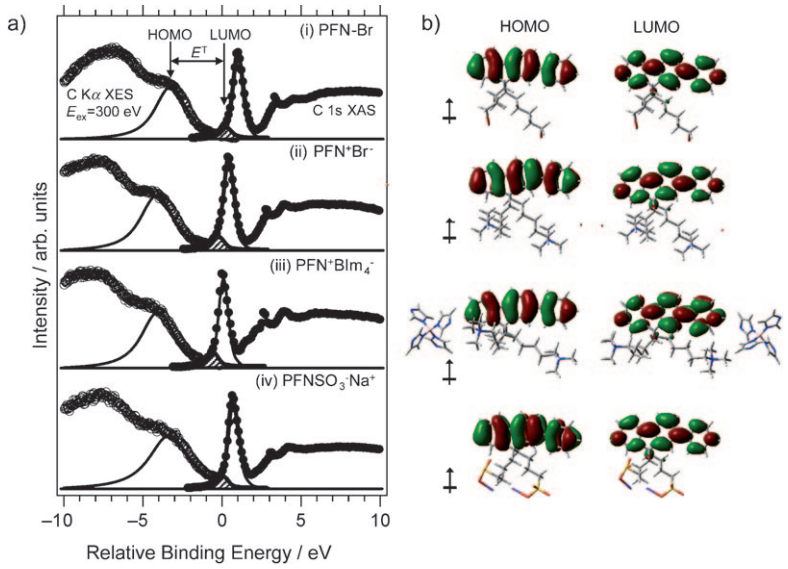

Figure 3. a) C Kα XES spectrum (red) taken at the E_{ex} of 310 eV and C 1s XAS spectrum (blue) of four conjugated polymers. b) The charge density contours for corresponding to HOMO/LUMO level obtained from DFT calculation after geometry optimization of all polymers. The red and green colors describe positive and negative charges, respectively. The direction of the permanent dipole is denoted as an arrow.

(empty circle) spectra (excited at $E_{ex}=300$ eV) of a neutral polymer and the three CPEs. A detailed description of data analysis is discussed in the Experimental Section. Briefly, after proper deconvolution of the XAS and XES spectra, the HOMO and LUMO energy positions were determined from the maximum point of each peak.[13,20] E^T can be obtained from the peak-to-peak distance between the HOMO and LUMO features; see Table 1 for a summary of the resulting E^T and E^{opt} values. From Table 1, we observe that the $E^{exciton}$ for four polymers range from 0.51 ± 0.05 to 0.74 ± 0.05 eV, where the largest $E^{exciton}$ is obtained for **PFN-Br** (0.74 ± 0.05 eV), and the smallest $E^{exciton}$ for **PFN$^+$Bim$_4^-$** (0.51 ± 0.05 eV).

Table 1. The ionization potential (IP), electron affinity (EA), energy gap (E^0)[a] in a gas-phase, transport gap (E^T), polarization energy (E^P)[b], optical gap (E^{opt}), exciton binding energy ($E^{exciton}$)[c] and molecular dipole moment (***P***) of conjugated polyelectrolytes obtained from the experimental and theoretical results.

	PFN-Br	**PFN$^+$Br$^-$**	**PFN$^+$Bim$_4^-$**	**PFNSO$_3^-$Na$^+$**
IP [eV]	5.46	5.32	5.53	5.43
EA [eV]	1.19	1.10	1.77	1.58
E^0 [eV]	4.27	4.22	3.76	3.85
E^T [eV]	3.72 ± 0.05	3.67 ± 0.05	3.46 ± 0.05	3.60 ± 0.05
E^P [eV]	0.55 ± 0.05	0.55 ± 0.05	0.30 ± 0.05	0.25 ± 0.05
E^{opt} [eV]	2.98	2.96	2.95	2.95
$E^{exciton}$ [eV]	0.74 ± 0.05	0.71 ± 0.05	0.51 ± 0.05	0.65 ± 0.05
P [Debye]	3.42	7.46	9.36	9.93

[a] $E^0=$IP−EA; [b] $E^P=E^0-E^T$; [c] $E^{exciton}=E^T-E^{opt}$.

The $E^{exciton}$ values of CPEs are larger than that of neutral conjugated polymers reported in the literature, thus E^T cannot be derived from optical absorption measurements for polymer semiconductors. This situation stems from the molecular polarization and charge localization. When a charge carrier is created in a molecular solid, its field polarizes the surrounding molecules. The energy gap in the solid phase (E^T) is thus expected to be different with that in the gas phase (E^0). The E^0 is derived from the difference between the IP and the EA as shown in Figure 1a. Because of the polarization energy induced on the surrounding medium by the photoinduced hole, the hole energy shifts to lower energy, E^{P+} (upward toward E_{vac} in Figure 1a) with respect to the HOMO level of the isolated molecule. On the LUMO side, the polarization energy induced by the presence of electron shifts the electron-state energy to lower potential energy, E^{P-} (downward away from E_{vac} in Figure 1a) with respect to the LUMO level of an insolated molecule.[20] Therefore, the polarization energy (E^P) and the relation between E^0 and E^T are given by Equations (1) and (2)[13,20]

$$E^P = E^{P+} + E^{P-} \quad (1)$$

$$E^T = E^0 - E^P \quad (2)$$

Figure 3b shows the charge density contours for the corresponding HOMO/LUMO levels of the conjugated polymers studied here, as obtained from DFT calculations. The interesting feature is that the HOMO and LUMO of the four polymers predominantly originate from the identical poly(fluorene-*co*-phenylene) backbone. From DFT calculations and Equations (1) and (2), E^0 and E^P are determined and summarized in Table 1. **PFN-Br** and **PFN$^+$Br$^-$** exhibit same values of E^P (0.55 ± 0.05 eV), while the E^P of **PFN$^+$Bim$_4^-$** (0.3 ± 0.05 eV) is similar to that of **PFNSO$_3^-$Na$^+$** (0.25 ± 0.05 eV).

To extract the molecular dipole experimentally is challenging due to the disorder in the material,[22] however with the help of DFT calculations we calculate ***P*** for four polymers. The directions of ***P*** for all conjugated polymers are illustrated as a blue arrow, toward positive charge. This is also supported by the distribution of the Mulliken atomic charges (see Supporting Information).[23,24] All polymers have permanent dipoles pointed in the same direction. Charged polymers have relatively large ***P*** as compared to the neutral polymer. Among the four polymers, **PFN$^+$Bim$_4^-$** and **PFNSO$_3^-$Na$^+$** have the largest ***P*** (9.36 and 9.93 Debye, respectively). The neutral polymer, **PFN-Br** has the smallest ***P*** (3.42 Debye) followed by the **PFN$^+$Br$^-$** (7.46 Debye). One can conclude that CPEs exhibit much stronger ***P*** than the neutral polymer. Previous UPS results have revealed small interfacial dipoles for **PFN-Br** and **PFNSO$_3^-$Na$^+$**,

while relatively large interfacial dipoles for **PFN$^+$Br$^-$** and **PFN$^+$Blm$_4^-$**. The calculated ***P*** of **PFN-Br**, **PFN$^+$Br$^-$** and **PFN$^+$Blm$_4^-$** are then in good agreement with the UPS results, except for **PFNSO$_3^-$Na$^+$**. It can be suggested that the shift in the vacuum level at the CPE/Au interface observed by UPS is due to the interfacial dipole, as well as the permanent dipole of CPEs.[9] Consequently, the calculated ***P*** may offer quantitative information on the formation of the interfacial dipole layer.

On the basis of our analysis of the experimental results, there are substantial differences in the electronic structures of CPEs as a function of counterion and charge. Table 1 summarizes values derived from these experimental and theoretical studies, including the calculated ***P***. Our results show that the E^T, $E^{exciton}$ and ***P*** show significant differences depending on the type of pendant ionic groups. The energy gaps in a gas-phase (E^0) for CPEs are altered by modification of chemical structures. From XAS and XES measurements, the E^T values for the CPEs were found in the range of 3.49 ± 0.05 to 3.72 ± 0.05 eV, depending on the type of counterions and charges. A comparison of E^T and E^{opt} for CPEs gave $E^{exciton}$ in the range of 0.51 ± 0.05 to 0.74 ± 0.05 eV. The neutral polymer with the highest $E^{exciton}$ implies a localization of the electron–hole pair, while the **PFN-Blm$_4^-$** with the lowest $E^{exciton}$ is associated with a more delocalized state.

To summarize, the electronic structures of conjugated polymers with identical poly(fluorene-*co*-phenylene) backbone but with different pendant charges and counterions have been investigated by a combination of experimental and theoretical methods. The simultaneous investigation of the unoccupied and occupied electronic states obtained from XAS and XES reveals that the different functional groups give rise to CPEs with dissimilar electronic structures, such as the HOMO/LUMO levels, and E^T. Theoretical calculations show that E^0 values of the CPEs are smaller than that of the neutral polymer. Furthermore, the ***P***s of CPEs are much larger than that of neutral counterpart. The values for E^T, $E^{exciton}$ and ***P*** provided here as a function of molecular structure are essential for proper understanding of function in optoelectronic devices and should be incorporated into future molecular design of CPE materials.

Experimental Section

Solution concentrations of 1% for **PFN-Br** and 0.6% for **PFN$^+$Br$^-$**, **PFN$^+$Blm$_4^-$** and **PFNSO$_3^-$Na$^+$** were prepared in different solvents (chlorobenzene for **PFN-Br**, methanol for **PFN$^+$Br$^-$** and **PFN$^+$Blm$_4^-$**, a 2:1 mixture of methanol and water for **PFNSO$_3^-$Na$^+$**). The prepared polymer solutions were spin coated on top of SiO_2 substrate (2000 rpm for **PFN-Br**, 1000 rpm for **PFN$^+$Br$^-$** and **PFN$^+$Blm$_4^-$**, and 4000 rpm for **PFNSO$_3^-$Na$^+$** for 60 s). The thickness of all CPEs films was determined to be approximately 30 nm by atomic force microscopy (AFM). To avoid surface contamination, the samples were then transferred from the N_2-atmosphere drybox to the metal deposition chamber without exposing to air and capped with a thin Au layer of ~5 nm.

XAS and XES measurements were carried out at beamline 8.0.1 of the Advanced Light Source at the Lawrence Berkeley National Laboratory, using the total fluorescence yield (TFY) mode. Excitation energy for the resonant and nonresonant C Kα (2p→1s transition) emission spectra were selected at 284.7 and 310 eV. The measurement angle was maintained at 30° between the incident X-ray and the plane of sample's surface. All measured spectra are normalized to the number of photons falling on the sample monitored by a highly transparent gold mesh.

As a process of evaluation of E^T, the relative binding energies of XAS and nonresonant XES spectra were calibrated using the C 1s binding energies taken from X-ray photoelectron spectroscopy (XPS). The C 1s binding energies of four polymers are follow; 284.4 eV for **PFN-Br**, 285 eV for **PFN$^+$Br$^-$**, 285.4 eV for **PFN$^+$Blm$_4^-$**, and 284.8 eV for **PFNSO$_3^-$Na$^+$**.[25] To determine the HOMO and LUMO energy positions, the spectra were deconvoluted using a combination of Gaussian and Lorentzian functions. The rightmost peaks of C Kα XES are assigned to be the HOMO position of each CPE. Using a similar technique, the LUMO levels are determined from the first deconvoluted peak of C 1s XAS.

DFT calculations were performed using the Gaussian 03 package with the nonlocal hybrid Becke three-parameter Lee–Yang–Parr (B3LYP) function and the 6-31G(d) basis set to elucidate the HOMO and LUMO levels after optimizing the geometries of all CPEs using the same method.

Acknowledgements

We are grateful to Prof. Gap Soo Chang for technical support. The authors thank the NSF CAREER grant (DMR# 0547639) for the financial support.

Keywords: conjugated polyelectrolytes · density functional theory · electronic structures · X-ray absorption spectroscopy · X-ray emission spectroscopy

[1] a) C. Hoven, R. Yang, A. Garcia, A. J. Heeger, T.-Q. Nguyen, G. C. Bazan, *J. Am. Chem. Soc.* **2007**, *129*, 10976–10977; b) B. Walker, A. Tamayo, J. Yang, J. Z. Brzezinski, T.-Q. Nguyen, *Appl. Phys. Lett.* **2008**, *93*, 063302; c) Y. Zhang, Y. Xu, Q. Niu, J. Peng, W. Yang, X. Zhu, Y. Cao, *J. Mater. Chem.* **2007**, *17*, 992–1001; d) F. Huang, L. T. Hou, H. B. Wu, X. H. Wang, H. L. Shen, W. Cao, W. Yang, Y. Cao, *J. Am. Chem. Soc.* **2004**, *126*, 9845–9853; e) C. Hoven, A. Garcia, R. Yang, V. Crockett, A. Heeger, G. Bazan, and T.-Q. Nguyen, *Proc. Natl. Acad. Sci. USA* **2008**, *105*, 12730—12735; f) D. W. Steuerman, A. Garcia, R. Yang, T.-Q. Nguyen, *Adv. Mater.* **2008**, *20*, 528–534.

[2] a) J. Yang, A. Garcia, T.-Q. Nguyen, *Appl. Phys. Lett.* **2007**, *90*, 103514–103517; b) P. Taranekar, Q. Qiao, H. Jiang, I. Ghiviriga, K. S. Schanze, J. R. Reynolds, *J. Am. Chem. Soc.* **2007**, *129*, 8958–8959; c) T. Kawai, T. Yamaue, K. Tada, M. Onoda, S. H. Jin, S. K. Choi, K. Yoshino, *Jpn. J. Appl. Phys. Part 2* **1996**, *35*, L741.

[3] L. Edman, B. Liu, M. Vehse, J. Swensen, G. C. Bazan, A. J. Heeger, *J. Appl. Phys.* **2005**, *98*, 044502.

[4] a) B. Liu, B. S. Gaylord, S. Wang, G. C. Bazan, *J. Am. Chem. Soc.* **2003**, *125*, 6705–6714; b) D. T. McQuade, A. E. Pullen, T. M. Swager, *Chem. Rev.* **2000**, *100*, 2537–2574.

[5] a) R. Yang, H. Wu, Y. Cao, G. C. Bazan, *J. Am. Chem. Soc.* **2006**, *128*, 14422–14423; b) F. Huang, X. Wang, D. Wang, W. Yang, Y. Cao, *Polymer* **2005**, *46*, 12010–12011.

[6] a) K. Lee, J. Y. Kim, S. H. Park, S. H. Kim, S. Cho, A. J. Heeger, *Adv. Mater.* **2007**, *19*, 2445–2449; b) X. Gong, S. Wang, D. Moses, G. C. Bazan, A. J. Heeger, *Adv. Mater.* **2005**, *17*, 2053–2058.

[7] A. Garcia, R. Yang, Y. Jin, B. Walker, T.-Q. Nguyen, *Appl. Phys. Lett.* **2007**, *91*, 153502.

[8] Y.-S. Huang, S. Westenhoff, I. Avilov, P. Sreearunothai, J. M. Hodgkiss, C. Deleener, R. H. Friend, D. Beljonne, *Nat. Mater.* **2008**, *7*, 483–489.

[9] J. H. Seo, T.-Q. Nguyen, *J. Am. Chem. Soc.* **2008**, *130*, 10042–10043.

[10] B. K. Yap, R. Xia, M. Campoy-Quiles, P. N. Stavrinou, D. D. C. Bradley, *Nat. Mater.* **2008**, *7*, 376–380.

[11] J. Hwang, E.-G. Kim, J. Liu, J.-L. Brèdas, A. Duggal, A. Kahn, *J. Phys. Chem. C* **2007**, *111*, 1378–1384.
[12] a) Y. Gao, *Acc. Chem. Res.* **1999**, *32*, 247–255; b) W. R. Salaneck, M. Lögdlund, M. Fahlman, G. Greczynski, Th. Kugler, *Mater. Sci. Eng. R* **2001**, *34*, 121–146.
[13] a) I. G. Hill, A. Kahn, Z. G. Soos, Jr., R. A. Pascal, *Chem. Phys. Lett.* **2000**, *327*, 181–188; b) E. V. Tsiper, Z. G. Soos, W. Gao, A. Kahn, *Chem. Phys. Lett.* **2002**, *360*, 47–52.
[14] A. Köhler, D. Beljonne, *Adv. Funct. Mater.* **2004**, *14*, 11–18.
[15] H. Ishii, K. Sugiyama, E. Ito, K. Seki, *Adv. Mater.* **1999**, *11*, 605–625.
[16] a) H. Yamane, H. Honda, H. Fukagawa, M. Ohyama, Y. Hinuma, S. Kera, K. K. Okudaira, N. Ueno, *J. Electron Spectrosc. Relat. Phenom.* **2004**, *137–140*, 223–227; b) K. Seki, H. Yanagi, Y. Kobayashi, T. Ohta, T. Tani, *Phys. Rev. B* **1994**, *49*, 2760–2767.
[17] a) W. L. Yang, J. D. Fabbri, T. M. Willey, J. R. I. Lee, J. E. Dahl, R. M. K. Carlson, P. R. Schreiner, A. A. Fokin, B. A. Tkachenko, N. A. Fokina, W. Meevasana, N. Mannella, K. Tanaka, X. J. Zhou, T. Buuren, M. A. Kelly, Z. Hussain, N. A. Melosh, Z.-X. Shen, *Science* **2007**, *316*, 1460–1462; b) J. Genzer, E. J. Kramer, D. A. Fischer, *J. Appl. Phys.* **2002**, *92*, 7070–7079; c) H. Peisert, T. Schwieger, J. M. Auerhammer, M. Knupfer, M. S. Golden, J. Fink, P. R. Bressler, M. Mast, *J. Appl. Phys.* **2001**, *90*, 466—469.
[18] a) A. Augustsson, M. Herstedt, J.-H. Guo, K. Edström, G. V. Zhuang, Jr., P. N. Ross, J.-E. Rubensson, J. Nordgren, *Phys. Chem. Chem. Phys.* **2004**, *6*, 4185–4189; b) M. Magnuson, L. Yang, J.-H. Guo, C. Såthe, A. Agui, J. Nordgren, Y. Luo, H. Ågren, N. Johansson, W. R. Salaneck, L. E. Horsburgh, A. P. Monkman, *J. Electron Spectrosc. Relat. Phenom.* **1999**, *101–103*, 573–578; c) J. E. Downes, C. McGuinness, P.-A. Glans, T. Learmonth, D. Fu, P. Sheridan, K. E. Smith, *Chem. Phys. Lett.* **2004**, *390*, 203–207.
[19] O. Fuchs, M. Zharnikov, L. Weinhardt, M. Blum, M. Weigand, Y. Zubavichus, M. Bär, F. Maier, J. D. Denlinger, C. Heske, M. Grunze, E. Umbach, *Phys. Rev. Lett.* **2008**, *100*, 027801.
[20] D. R. T. Zahn, G. N. Gavrila, G. Salvan, *Chem. Rev.* **2007**, *107*, 1161–1232.
[21] a) E. Ettedgui, H. Razafitrimo, Y. Gao, B. R. Hsieh, W. A. Feld, M. W. Ruckman, *Phys. Rev. Lett.* **1996**, *76*, 299–302; b) L. R. Pattison, L. R. Pattison, A. Hexemer, E. J. Kramer, S. Krishnan, P. M. Petroff, D. A. Fischer, *Macromolecules* **2006**, *39*, 2225–2231.
[22] J. Park, R. Yang, C. V. Hoven, A. Garcia, D. A. Fischer, T.-Q. Nguyen, G. C. Bazan, D. M. DeLongchamp, *Adv. Mater.* **2008**, *20*, 2491–2496.
[23] H. Lüth, *Surface and interfaces of solid materials*, Springer, Berlin, **1995**, p. 509.
[24] a) S. W. Cho, Y. Yi, J. H. Seo, C. Y. Kim, M. Noh, K.-H. Yoo, K. Jeong, C.-N. Whang, *Synth. Met.* **2007**, *157*, 160–164; b) R. Sarangi, J. T. York, M. E. Helton, K. Fujisawa, K. D. Karlin, W. B. Tolman, K. O. Hodgson, B. Hedman, E. I. Solomon, *J. Am. Chem. Soc.* **2007**, *130*, 933–937.
[25] J. H. Seo, R. Yang, J. Z. Brzezinski, B. Walker, G. C. Bazan, T.-Q. Nguyen, *Adv. Mater.*, in press.

Received: November 12, 2008
Published online on February 19, 2009

